

Human umbilical cord-derived mesenchymal stem cells spontaneously form 3d aggregates and differentiate in an embryoid body-like manner

Abstract

Human adult mesenchymal stem cells (hMSC) are particularly suitable cells for autologous tissue engineering and cell-based therapies. They can be isolated from various tissues, such as bone marrow, adipose tissue, dental pulp or umbilical cords. Due to their primitive developmental stage, umbilical cord-derived hMSC are assumed to have a higher proliferation and differentiation capacity than hMSC from adult tissues. We isolated hMSC from bone marrow (BM) and umbilical cords (UC) and compared the cells regarding their surface epitopes, proliferation and differentiation capacity.

Flow cytometry of specific surface epitopes showed that both BM-MSC and UC-MSC display the characteristic MSC phenotype. Cells from both sources were readily differentiated into adipocytes, osteoblasts and chondrocytes according to standard protocols. Interestingly, only UC-MSC spontaneously formed three-dimensional aggregates when cultured under post-confluent conditions. The cells of these aggregates were viable and spontaneously differentiated into several specialized cell types akin to the well-known differentiation of embryoid bodies. Besides, UC-MSC expressed the pluripotency-associated gene NANOG as well as genes characteristic for the mesodermal and ectodermal fate. Thus, UC-MSC resemble BM-MSC but additionally show a spontaneous embryoid body-like aggregation and differentiation *in vitro*. These results indicate that UC-MSC are less restricted than BM-MSC and may thus extend the limits of BM-MSC based therapies.

Keywords: human adult mesenchymal stem cells, autologous tissue engineering, bone marrow, cardiomyocytes, umbilical cord stem cells

Volume 1 Issue 5 - 2016

Adamzyk C,^{1,2} Labude N,¹ Schneider RK,¹ Jaekel J,¹ Hoffmann V,¹ Fischer J,^{1,2} Hoss M,³ Knuechel R,¹ Jahnen Dechent W,² Neuss S^{1,2}

¹Institute of Pathology, RWTH Aachen University, Germany
²Helmholtz Institute for Biomedical Engineering, RWTH Aachen University, Germany
³Electron Microscopic Facility, RWTH Aachen University, Germany

Correspondence: Sabine Neuss, Institute of Pathology and Helmholtz Institute for Biomedical Engineering, Biointerface Group, RWTH Aachen University, Pauwelsstr 30, 52074 Aachen, Germany, Tel +49 241 8080622, Fax +49 241 8082439, Email sneuss-stein@ukaachen.de

Received: October 31, 2016 | **Published:** November 17, 2016

Abbreviations: hMSC, human adult mesenchymal stem cells; BM, bone marrow; UC, umbilical cords

Introduction

In modern medicine, embryonic and adult stem cells are important tools to develop future cell-based therapies or innovative tissue engineering applications. Both cell types show advantages and disadvantages. Embryonic stem cells are subjected to ethical concerns and teratogenic risks but have a high proliferation potential and can differentiate towards all cell types of the three germ layers. In contrast, adult stem cells are more restricted in their proliferation and differentiation capacity but can be used for autologous applications without ethical concerns and teratogenic potential. A cell type combining pluripotency and proliferative capacity of embryonic stem cells but lacking the ethical concerns and teratogenicity would be ideal for tissue engineering and cell-based therapies.

Since the breakthrough of reprogramming somatic cells into induced pluripotent stem cells (iPSC) by Takahashi & Yamanaka in 2006¹ many stem cell research groups recently focus on these patient-specific pluripotent stem cells for future therapies. However, due to their pluripotent state, a teratogenic risk cannot be excluded.

Human adult mesenchymal stem cells (hMSC) can be isolated from various tissues, such as bone marrow (BM), adipose tissue, dental pulps or umbilical cords (UC). Due to their primitive developmental stage, umbilical cord-derived hMSC are assumed to

have a higher proliferation and differentiation capacity than hMSC from other adult donor sources. Umbilical cord stem cells are readily available at birth and no ethical concerns are subjected to this cell type. UC-MSC show both high self-renewing and differentiation capacity. Several publications describe the differentiation of UC-MSC into mesenchymal lineages, such as adipocytes, osteoblasts, chondrocytes,²⁻⁴ cardiomyocytes,^{5,6} endothelial cells^{7,8} and skeletal myocytes,⁹ as well as differentiation across the mesodermal germ layer. Besides the differentiation into ectodermal cells, such as (dopaminergic) neurons,^{2,10-12} the differentiation into endodermal cells, e.g. insulin-producing cells⁶ or in particular into functional hepatocytes, was reported.¹³⁻¹⁵ Furthermore, UC-MSC share their gene expression profile with adult bone marrow-derived hMSC (BM-MSC) and with embryonic stem cells,¹⁶⁻¹⁸ exhibit a non-immunogenic phenotype like BM-MSC^{19,20} and do not induce teratomas when transplanted into SCID mice.^{21,22} Thus, UC-MSC exhibit an intermediate cell type between embryonic and adult stem cells and combining their respective advantages.

Studies comparing UC-MSC with BM-MSC^{2-4,23} and the results presented in this work confirm the resemblance of both cell types. Additionally, we describe a striking phenomenon distinguishing UC-MSC from BM-MSC and supporting the theory that UC-MSC are intermediate between embryonic and adult stem cells: the spontaneous three-dimensional embryoid body-like aggregation and multilineage differentiation, when cultured under post-confluent conditions.

Materials and methods

Isolation and expansion of hMSC

Human mesenchymal stem cells were isolated after informed consent and approval of the local Ethics Committee from femoral head spongiosa (bone marrow) and umbilical cord Wharton's Jelly. Isolation of BM-MSC was accomplished as previously described.²⁴⁻²⁸ In brief, after rinsing the spongiosa with stem cell medium several times, spongiosa was removed and the remaining cell suspension was centrifuged for 10 min at 500xg. Thereafter, the cell pellet was resuspended in stem cell medium and cells were seeded in a T75 culture flask and cultured at 37°C in a 20% O₂ and 5% CO₂ humidified atmosphere. After 24 hours, non adherent (hematopoietic) cells were removed by medium change.

Isolation of UC-MSC was performed according to the protocol of Wang and coworkers.²⁹ Briefly, the umbilical cord was cut into pieces 2cm long and then opened lengthwise using a scalpel. The Wharton's Jelly was scraped out and arteries and vein were removed. Next, the Wharton's Jelly was incubated over night in 10ml collagenase/DMEM solution (172 I.U./ml, Worthington, Lakewood NJ, USA). After addition of 30ml stem cell medium (PAN Biotech, Aidenbach, Germany) and after vortexing, the suspension was centrifuged for 10min at 500xg. The resulting cell pellet was digested in 10ml trypsin solution (2.5%, Sigma, Steinheim, Germany) at 37°C for 30min. Again, 30ml stem cell medium were added, vortexed, and centrifuged for 10min at 500xg. After washing twice with 20ml stem cell medium, the cell pellet was resuspended in 10ml stem cell medium and cells were seeded in a T75 culture flask and cultured at 37°C in a 20% O₂ and 5% CO₂ humidified atmosphere. After 24 hours, non adherent (hematopoietic) cells were removed by medium exchange. Mesenchymal stem cells from bone marrow (BM-MSC) and umbilical cord Wharton's Jelly (UC-MSC) were expanded in stem cell medium (PAN Biotech, Aidenbach, Germany) consisting of 60% DMEM low glucose and 40% MCDB-201 supplemented with 2% FCS, 1xITS-plus (insulin-transferrin-selenic acid+BSA-linoleic acid), 1nM dexamethasone, 100µM ascorbic-acid-2-phosphate, and 10ng/ml EGF. Medium was changed every 3-4 days. At 80-90% confluence, stem cells were trypsinized with stem cell trypsin (CellSystems, St. Katharinen, Germany) and reseeded in a density of 5,000cells/cm² for optimal proliferation. Additionally, MSC were grown under post-confluent conditions for up to 6 weeks. Here, post-confluent condition means that MSC were not passaged when 80-90% confluence was reached, but further cultured for up to 6 weeks. All UC-MSC cultures, but no BM-MSC cultures spontaneously aggregated into macroscopically visible cell clusters.

Differentiation of hMSC into adipocytes, osteoblasts and chondrocytes

To demonstrate the multipotency of isolated BM-MSC and UC-MSC, cells were induced to differentiate into adipocytes, osteoblasts and chondrocytes following standard protocols.³⁰ For adipogenic differentiation, cells were seeded in a density of 8x10⁴ cells/cm² in stem cell medium. Then, the medium was changed every 3-4 days alternately from adipogenic induction to adipogenic maintenance medium for 21 days. The adipogenic induction medium consisted of DMEM high glucose (PAA Laboratories, Cölbe, Germany) with 1µM dexamethasone, 0.2mM indomethacin, 0.01mg/ml insulin, 0.5mM 3-isobutyl-1-methyl-xanthine (all Sigma, Steinheim, Germany), and 10% FCS (PAN Biotech). The adipogenic maintenance medium was

composed of DMEM high glucose (PAA) with 0.01mg/ml insulin (Sigma) and 10% FCS (PAN Biotech). After 21 days, cells were fixed with 90% ethanol and stained for 10min with Oil red O solution (Sigma) to visualize lipid vacuoles.

For osteogenic differentiation, cells were seeded in a density of 3.1x10⁴cells/cm² and stimulated with osteogenic induction medium for 21 days. The medium consisted of DMEM low glucose (PAA), 10% FCS (PAN Biotech), 100nM dexamethasone, 10mM sodium β-glycerophosphate, and 0.05mM L-ascorbic acid 2-phosphate (all Sigma) and was replaced every 2-3 days. After 21 days of differentiation, cells were fixed with 70% ethanol for 1hour, washed with aqua bidest, and stained with Alizarin red solution (40mM, pH 4.1, Sigma) for 10min. Stained cells were washed three times with phosphate-buffered saline (PBS), and calcium deposits were visible.

For chondrogenic differentiation, 0.5ml cell suspension (5x10⁵cells/ml) was placed into a 15ml polypropylene tube (Becton Dickinson, Heidelberg, Germany) and centrifuged for 10min at 500xg to obtain cell pellets. The pellets were cultured in serum-free chondrocyte induction medium consisting of DMEM high glucose (PAA), 100nM dexamethasone, 0.17mM L-ascorbic acid 2-phosphate, 100µg/ml sodium pyruvate, 40µg/ml proline (all Sigma, Steinheim, Germany), and 1% ITS-plus (Becton Dickinson, Heidelberg, Germany). TGF-β₃ (R&D Systems, Wiesbaden, Germany) was added in a concentration of 10ng/ml medium at each medium change. After 21 days, pellets were formalin fixed and paraffin embedded. Thin sections were stained with Toluidin blue (Sigma) to visualize proteoglycans in the extracellular matrix.

Proliferation

To measure cell proliferation, BM-MSC and UC-MSC were seeded in 96-well plates in a density of 3,000cells/cm². Metabolic activity was analyzed at six time points after cell seeding. Therefore, the XTT Cell Proliferation KitII from Roche was used according to the manufacturers' instructions (Roche, Mannheim, Germany).

Flow cytometry

For flow cytometry, 2.5x10⁵ cells were preincubated at 4°C for 30min in 100µl PBS containing 1% bovine serum albumin (BSA). 1µg primary antibody was added for further 60min at 4°C. Cells were washed three times in 100µl PBS containing 0.1% BSA and resuspended in PBS containing 1% BSA. This was followed by an incubation with the secondary antibody (1:20 dilution) in PBS/1% BSA for 45min at 4°C in the dark. Again, cells were washed as previously described and resuspended in 100µl PBS. The monoclonal mouse antibodies CD4, CD14, CD73, CD90 were purchased from BD Biosciences (Heidelberg, Germany), CD105 from R&D Systems (Wiesbaden-Nordenstadt, Germany) and the corresponding secondary antibody (conjugated with fluorescein isothiocyanate) from DAKO (Glostrup, Denmark). Species-matched immunoglobulin Gs (IgGs) served as negative control. Data of 10,000 stained cells were collected and analyzed using a FACSCalibur instrument and FACSCalibur software (Becton Dickinson, Heidelberg, Germany).

Immunohistochemistry of BM-MSC and UC-MSC

The medium was removed and cells were washed with PBS, followed by a fixation in 4% paraformaldehyde for 30 minutes. Thereafter, cells were washed again three times with PBS and preincubated for 1 hour in a permeabilisation solution containing

Triton X-100 (0.5%, Sigma) and 3% normal horse serum (NHS). Solution was removed and replaced by the primary antibodies CK 5/6 (1:100, mouse monoclonal), CK 10/13 (1:50, mouse monoclonal), pan-CK (clone AE1/AE3, 1:50, mouse monoclonal), NSE (1:800, mouse monoclonal), vimentin (1:10, mouse monoclonal, all DAKO) or *NANOG* (1:50, rabbit monoclonal, Lifespan Biosciences, Seattle, USA) diluted in PBS with 3% NHS for overnight incubation. After three washing steps with PBS, the cells were incubated with the secondary antibody Alexa 488 (1:400, donkey anti-mouse IgG; molecular probes, invitrogen detection techniques, Eugen, Orgeon, USA) or with the secondary antibody Cy3 (1:200, goat anti rabbit, Jackson ImmunoResearch, Suffolk, UK) diluted in PBS with NHS. Genomic DNA was then labeled with a DAPI solution in PBS for additional 15 minutes before final washes and mounting with Immu-Mount (Thermo Electro Corporation, Pittsburgh, PA).

Histology and immunohistochemistry of three-dimensional aggregates

For histological analysis UC-MSC-derived 3D aggregates were fixed in 3.7% formaldehyde for 24h, paraffin embedded, orientated on the perpendicular plane and cut with a rotating microtome at 3µm thickness (Leica, Wetzlar, Germany). Sections were stained with hematoxylin and eosin (Sigma) according to routine histology protocols.

For immunohistochemistry, cryosections of UC-MSC-derived 3D aggregates were fixed for 30 min using 0.5% paraformaldehyde (in PBS). After washing with 0.5% BSA in PBS, unspecific protein-binding capacity was blocked for 15 min using blocking buffer (5% BSA in PBS). Sections were incubated for 45 min at RT with the primary antibody (1:50 dilution in 1:200 dilution of NP-40 in 0.5% BSA/PBS), washed three times for 10 min in 0.5% BSA/PBS, followed by an incubation with the secondary antibody (1:250 in 0.5% BSA/PBS) for 30 min at RT protected from light. Again, sections were washed for three times as previously described. The monoclonal mouse antibodies vimentin, pan-cytokeratin and Ki-67 and the secondary antibodies (conjugated with DAB or fluorescein isothiocyanat) were purchased from DAKO. Species-matched immunoglobulin Gs (IgGs) served as negative control.

Transmission electron microscopy

Samples were fixed in 3% glutaraldehyde (in 0.1 M Soerensen's phosphate buffer (pH 7.4; 13mM NaH₂PO₄·xH₂O; 87mM Na₂HPO₄·x2H₂O) for 14 hours, washed with 0.1M Soerensen's phosphate buffer overnight, followed by 1h in 1% OsO₄ (in 17% sucrose buffer (pH 7.4; 88ml 0.1M Soerensen's phosphate buffer; 12ml aqua dest., 17g sucrose), rinsed with water and dehydrated with ethanol (30%-100%) and propylenoxide (100%). Finally samples were processed for embedding in Epon, polymerized 8h at 37°C and 56h at 60°C, cut into 70-100nm thick slices and contrasted with uranyl acetate and lead citrate. The samples were analyzed with a PHILIPS EM 400T at 60kV and micrographs were taken by an OLYMPUS CCD-Camera MORADA.

Reverse transcriptase polymerase chain reaction

Total RNA of BM-MSC and UC-MSC was extracted using the RNeasy RNA purification kit (Qiagen, Hilden, Germany), based on a guanidinium thiocyanate method according to the manufacturers' instructions. The RNA concentration was measured spectrophotometrically using the Nanodrop System (Thermo Fisher

Scientific, Schwerte, Germany). Remaining genomic DNA was digested with DNaseI from bovine pancreas (10.000 units, Roche, Mannheim, Germany) by incubation at 37°C for 1hour (1µl DNaseI / 30µg RNA). Reverse transcription was carried out with 5µg of total RNA using the High-Capacity RNA-to-cDNA Master Mix (Applied Biosystems, Darmstadt, Germany) according to the manufacturers' instructions.

For polymerase chain reaction, 0.5µl primer forward (20pmol/µl, MWG, Ebersberg, Germany), 0.5µl primer reverse (20pmol/µl, MWG), 1µl dNTPs (10mM each dNTP), 0.5µl Taq polymerase, 5µl 10x buffer (including MgCl₂, all Roche, Mannheim, Germany) and 41.5µl H₂O (RNase free) were mixed. As a template, 1µl cDNA was added. Instead of cDNA, 1µl H₂O served as a negative control. The following temperature cycles were repeated 35 times to amplify specific cDNA sequences: denaturation at 95°C for 1min, annealing at 60°C for 1min, and extension at 72°C for 1min. Finally, an extension step (72°C for 10min) was accomplished. PCR product size was analyzed by electrophoresis (2% agarose gel, 100mV, 50min) and visualized with ethidium bromide. A 100bp DNA ladder (Invitrogen, Karlsruhe, Germany) served as a marker. Primer sequences were used as follows: *NANOG* forward: 5'-AGTCCCAAAGGCAAACAACCCACTTC-3' *NANOG* reverse: 5'-TGCTGGAGGCTGAGGTATTCTGTCTC-3' (product size: 164bp).

Results

Characterization of hMSC derived from bone marrow and umbilical cord Wharton's Jelly

Human MSC from both sources, bone marrow (BM-MSC) and umbilical cord Wharton's Jelly (UC-MSC) are similar in their standard differentiation capacity and surface epitope expression. The cells can be differentiated *in vitro* into adipocytes, osteoblasts and chondrocytes Figure 1A following established protocols.³⁰ In general, UC-MSC show a higher differentiation capacity towards osteoblasts than towards adipocytes. The lipid vacuoles of UC-MSC are less in size and number compared to lipid vacuoles of BM-MSC (Figure 1A). As shown by flow cytometry, UC-MSC and BM-MSC both express the characteristic surface epitopes CD73, CD90, and CD105 and do not express hematopoietic markers, such as CD4 and CD14 (Figure 1B).

Proliferation capacity of BM-MSC and UC-MSC

Figure 2 demonstrates the viability of hMSC at six different time points. UC-MSC show a higher proliferation capacity than BM-MSC. The mean population doubling time is 6.45 days for the BM-MSC, and only 3.32 days for the UC-MSC.

Spontaneous 3D aggregation and multilineage differentiation of UC-MSC

When cultured under post-confluent conditions for up to 6 weeks, we observed a spontaneous three-dimensional aggregate formation of UC-MSC in each cell isolate (n>40) and each passage (P0-P4). None of the BM-MSC cultures showed this phenomenon at any time point. The 3D aggregates of UC-MSC are up to 7mm (49mm²) in size (Figure 3A). They are redolent of embryoid bodies and consist of different types of specialized cells (Figure 3). The HE staining displays tissue-like structures embedded in extracellular matrix Figure 3B and an epithelial-like boundary Figure 3C. Within the aggregates, histological stainings, such as oil red o, alizarin red and toluidin blue

reveal clusters of differentiated cells, like adipocytes, osteoblasts, and chondrocytes, respectively, (Figure 3D & 3F). Comparable to differentiation processes in embryoid bodies, the different cell types within the UC-MSC-derived aggregates appear in clusters and are not uniformly distributed. The lipid vacuoles of the spontaneously derived adipocytes are even larger than the vacuoles of the induced UC-MSC adipocytes (compare Figure 1A with Figure 3D). The expression of the mesenchymal marker vimentin infers from the mesenchymal origin of the cells (Figure 3G). Besides a mesodermal fate, some cells in the aggregates display an ectodermal fate, represented by clusters of pan-cytokeratin positive cells (Figure 3H) or clusters of

neuron specific enolase (NSE) positive cells (Figure 3I). However, E-Cadherin, an early epithelial marker and adhesion protein, and von Willebrand-Factor, a protein expressed by endothelial cells could not be detected (not shown). α -fetoprotein, an endodermal marker, S100 and glial fibrillary acid protein (ectodermal markers) were also not expressed in the aggregates (not shown). Due to a low proliferation index (<3% of Ki67 positive cells) an aberrant or tumorigenic growth can be excluded for the cells inside the three-dimensional aggregates (Figure 3J). The electron microscopic view on the aggregates displays compact layers of flattened cells (Figure 3K). Most of the cells include large numbers of multilamellar bodies, as shown in Figure 3L.

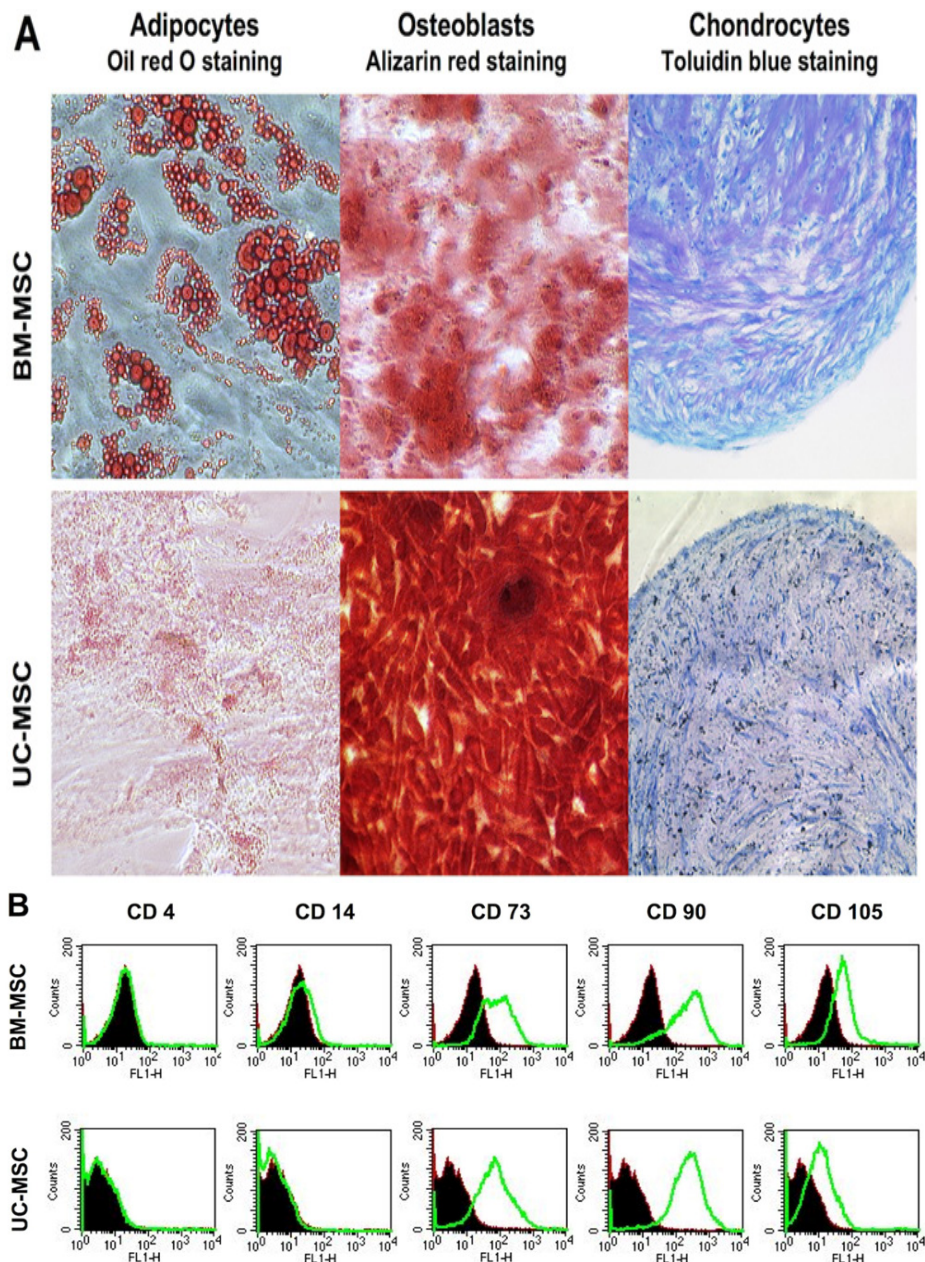


Figure 1 Characterization of hMSC.

Multipotency and surface marker characterization of hMSC, according to the minimal criteria of the International Society for Cellular Therapy.³² A) Stem cells were differentiated into adipocytes, osteoblasts, and chondrocytes using established *in vitro* differentiation protocols. The success of differentiation is demonstrated by histological stainings, oil red O, alizarin red, and toluidin blue, respectively. B) The cells express the surface epitopes CD105, CD90, and CD73, but no hematopoietic markers, such as CD4 and CD14. Thus, cell types, BM-MSC (above), and UC-MSC (below) meet the minimal criteria for MSC characterization. Magnification: 200x (adipocytes, osteoblasts); 100x (chondrocytes).

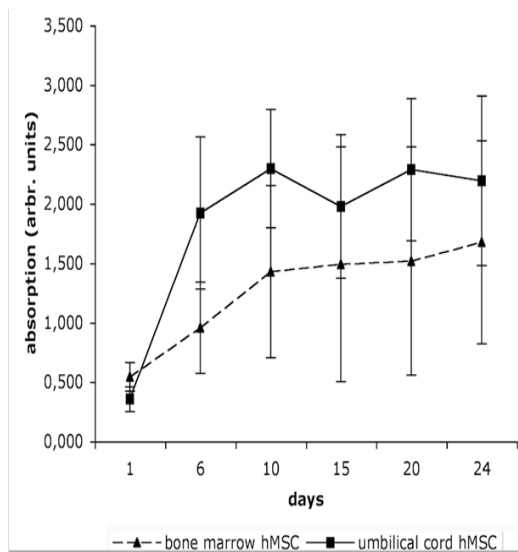


Figure 2 Proliferations of BM-MSC and UC-MSC.

The proliferation of hMSC was analyzed by XTT cell viability measurements at six different time points (day 1, 6, 10, 15, 20, 24]. Both BM-MSC and UC-MSC showed donor variation, but nevertheless twice the proliferation rate in UC-MSC than in BM-MSC (n=5).

Basal expression of ectodermal genes in UC-MSC

To analyze, whether UC-MSC in three-dimensional aggregates spontaneously differentiated into pan-cytokeratin positive cells or whether they expressed cytokeratins before aggregation, we performed immunohistochemistry. Our results for subconfluent UC-MSC and BM-MSC confirmed the mesenchymal origin of both cell types demonstrated by a strong vimentin signal (Figure 4). In contrast to BM-MSC, UC-MSC expressed early and basal cytokeratins (cytokeratin 5,6 and cytokeratin 10,13, respectively) (Figure 4). Thus, ectodermal markers were already expressed before UC-MSC aggregation.

Expression of the pluripotency-associated gene NANOG in UC-MSC

NANOG is a pluripotency-associated gene expressed in embryonic stem cells and induced pluripotent stem cells. Figure 5 shows that NANOG was not expressed in BM-MSC, but the protein was readily detected in UC-MSC and UC-MSC-derived aggregates (Figure 5A-5C). On the RNA level, *NANOG* transcripts were likewise detectable in UC-MSC cells and UC-MSC-derived aggregates, but not for BM-MSC (Figure 5D).

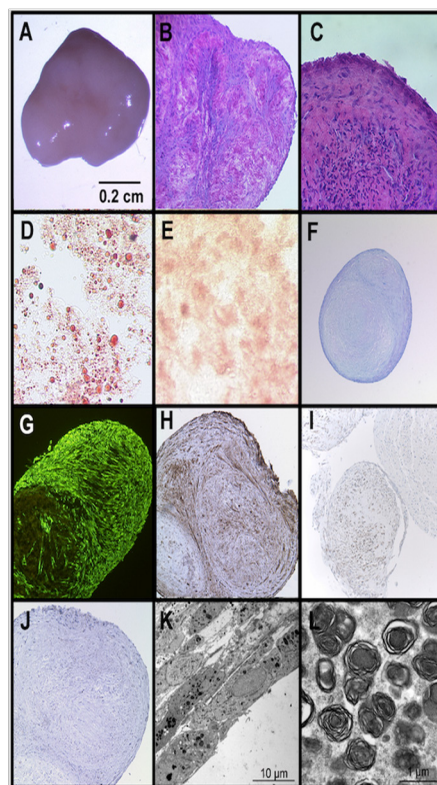


Figure 3 Three-dimensional aggregation and spontaneous differentiation of UC-MSC.

Mesenchymal stem cells from umbilical cord, but not from bone marrow spontaneously formed three-dimensional aggregates *in vitro*, when cultured under post-confluent conditions. The aggregates had up to 7mm (49mm²) cross-sectional area at their largest circumference (A). HE staining of sectioned aggregates demonstrates vital, not necrotic areas in the centre of these aggregates (B). In addition complex, tissue-like structures with epithelial morphology were present at the margins of the aggregates (C). Oil red O staining, alizarin red staining and toluidin blue staining demarcated clusters of cells within the aggregates, which were differentiated into adipocytes (D), osteoblasts (E) and chondrocytes (F), respectively. Immunohistochemistry indicated the mesenchymal origin of the UC-MSC by a strong vimentin expression (G), but also visualized clusters of ectodermal cells by pan-cytokeratin expression (H) and NSE expression (I). The weak Ki67 (J) staining (positive cells <3%) indicates a low proliferating growth of aggregates. Transmission electron microscopy shows compact layers of UC-MSC in 3D aggregates (K). Most of the cells included in the 3D aggregates show high numbers of multilamellar bodies suggesting extensive remodelling in the aggregates (L). Magnification: B, C, G-J: 100x; F: 50x; D, E: 200x.

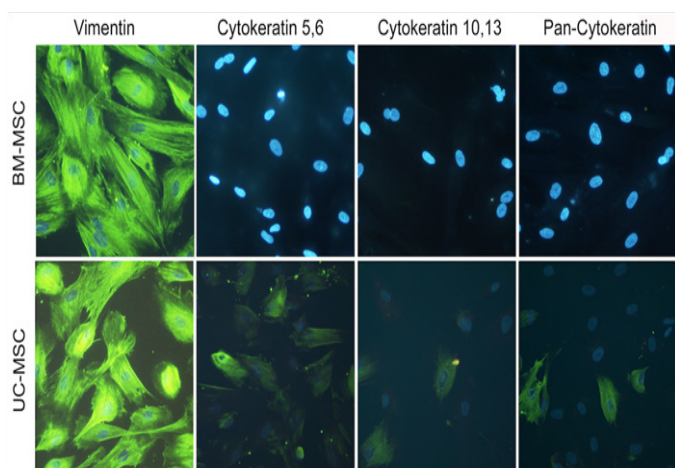


Figure 4 UC-MSC express ectodermal proteins.

Immunohistochemistry revealed subpopulations of UC-MSC expressing the early ectodermal markers cytochrome 5,6 and the mature ectodermal markers cytochrome 10,13. In contrast, BM-MSC did not express any of the tested ectodermal markers. Both MSC types were strongly positive for the mesenchymal marker vimentin. Magnification: 200x.

“Younger“ tissue, such as the umbilical cord, is supposed to accommodate hMSC with higher self-renewal and differentiation capacity than “older“ tissue,²¹ such as bone marrow or adipose tissue. Numerous studies report on the comparison of “younger“ UC-MSC and “older“ BM-MSC.^{2,13,23,31} These studies anticipated our result that UC-MSC proliferated about twice stronger than BM-MSC with population doubling times of 3.32 and 6.45 days, respectively (Figure 2). Further, the multipotency of both cell types was confirmed by differentiation into adipocytes, osteoblasts, and chondrocytes, although as a general rule, the UC-MSC derived adipocytes had smaller and fewer lipid vacuoles than the BM-MSC (Figure 1A). Both BM-MSC and UC-MSC thus met the minimal criteria positioned by the International Society for Cellular Therapy to be referred to as MSC.³² Besides the mesodermal fate, UC-MSC are able to differentiate across the germ layers e.g. into neurons,^{2,10} endothelial cells,⁷ and into hepatocytes expressing hepatic markers, and even store glycogen and produce urea.¹³ Campard and coworkers described the constitutive expression of endodermal proteins, like albumin, cytochrome 19 and connexin-32.¹³ This initial constitutive expression of lineage markers is in accordance to our results. We could detect the early epidermal markers cytochrome 5,6 and the mature epidermal markers cytochrome 10,13 in subpopulations of UC-MSC. The co-expression of the mesenchymal marker vimentin with these ectodermal proteins is indicative for cells undergoing epithelial-mesenchymal transition as it is described e.g. for cells involved in embryonic development. Such induction/transition processes allow for a switching between two cell states, the adherent epithelial cells and the migratory mesenchymal cells and thus are essential to build up complex organ structures.³³

Besides lineage markers, UC-MSC share expressed genes with embryonic stem cells e.g. OCT-4, SOX-2, NANOG, DNMT3B and GABRB3.^{14,16,34} Here we demonstrated a NANOG expression on the RNA and protein level for UC-MSC but not for BM-MSC (Figure 5). NANOG is critically required for the acquisition of both embryonic and induced pluripotency.³⁵ Thus, NANOG may mediate pluripotency in UC-MSC as well.

Despite the expression of the pluripotency marker NANOG, UC-MSC are generally considered as adult stem cells, which retain their original phenotype during *in vitro* expansion and do not undergo spontaneous differentiation.^{2,17,31} In contrast, we here describe for the first time a spontaneous embryoid body-like three-dimensional aggregation and differentiation of UC-MSC, when cultured under post-confluent conditions. The aggregates are macroscopically visible and up to 7 mm in size. Their tissue-like structure contains diverse clusters of differentiated cells, such as adipocytes, osteoblasts and chondrocytes Figure 3D-3H, but does not show a tumorigenic growth potential (Figure 3I). Many cells within the aggregates include high amounts of multilamellar bodies (Figure 3J-3L). These organelles store lipids and have secretory functions. Multilamellar bodies are detectable in cells covering surfaces, such as skin, lung alveolae, tongue papillae, oral epithelium or the mucosa of the stomach. They secrete specialized lipid components, often resulting in a protective lining against environmental influences. Lamellar bodies also occur in mesodermal cell layers of sliding surfaces, such as the peritoneum, pericardium or pleural mesothelium.³⁶ The formation of the UC-MSC-derived three-dimensional aggregates probably involves sliding processes and lipid components secreted by multilamellar bodies might facilitate the development of three-dimensional structures and additionally result in a protective layer against the environment.

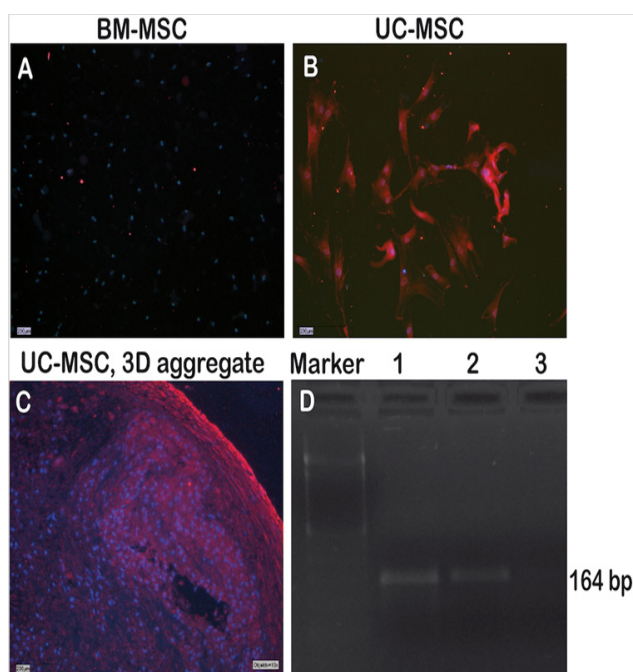


Figure 5 UC-MSC express the pluripotency gene NANOG.

The pluripotency-associated gene NANOG was not expressed in BM-MSC (A), but was present in UC-MSC and in UC-MSC-derived three-dimensional aggregates (B,C). PCR results (D) verified the expression of NANOG transcripts in UC-MSC (lane 1) and UC-MSC-derived aggregates (lane 2), but not in BM-MSC (lane 3).

Discussion

Human mesenchymal stem cells (hMSC) from different origins are considered as a useful cell source for tissue engineering and regenerative medicine. However, their multipotent differentiation capacity is restricted to the mesenchymal cell lineage in contrast to pluripotent embryonic stem cells or induced pluripotent stem cells.

In summary, UC-MSC share characteristics with BM-MSC but additionally they (i) express the pluripotency-associated gene NANOG, (ii) show characteristics for epithelial mesenchymal transition, (iii) spontaneously form three-dimensional aggregates akin to embryoid bodies, (iv) start to differentiate during aggregate formation and (v) have large amount of multilamellar bodies, which probably support the aggregation process.

Conclusion

The present study demonstrates for the first time a spontaneous aggregation and multilineage differentiation of UC-MSC, comparable to the embryoid body formation of embryonic stem cells. Our data support the hypothesis, that Wharton's Jelly derived umbilical cord hMSC may have a higher proliferation and differentiation capacity and may thus be less restricted stem cells than hMSC from bone marrow or adipose tissue. Thus, Wharton's Jelly derived umbilical cord hMSC may represent an ideal cell source for cell-based therapies and tissue engineering applications.

Acknowledgements

We thank Stephanie Brosig for technical assistance, the Department of Orthopedic Surgery (RWTH Aachen University) for providing bone spongiosa and the Department of Obstetrics and Gynecology (RWTH Aachen University) for providing umbilical cords.

Conflict of interest

The author declares no conflict of interest.

References

1. Takahashi K, Yamanaka S. Induction of pluripotent stem cells from mouse embryonic and adult fibroblast cultures by defined factors. *Cell*. 2006;126(4):663–676.
2. Karahuseynoglu S, Cinar O, Kilic E, et al. Biology of stem cells in human umbilical cord stroma: *in situ* and *in vitro* surveys. *Stem Cells*. 2007;25(2):319–331.
3. Baksh D, Yao R, Tuan RS. Comparison of proliferative and multilineage differentiation potential of human mesenchymal stem cells derived from umbilical cord and bone marrow. *Stem Cells*. 2007;25(6):1384–1392.
4. Harris DT. Umbilical cord tissue mesenchymal stem cells: characterization and clinical applications. *Curr Stem Cell Res Ther*. 2013;8(5):394–349.
5. Kadivar M, Khatami S, Mortazavi Y, et al. *In vitro* cardiomyogenic potential of human umbilical vein-derived mesenchymal stem cells. *Biochem Biophys Res Commun*. 2006;340(2):639–647.
6. Wang L, Ott L, Seshareddy K, et al. Musculoskeletal tissue engineering with human umbilical cord mesenchymal stromal cells. *Regen Med*. 2011;6(1):95–109.
7. Wu KU, B Zhou, SH Lu, et al. *In vitro* and *in vivo* differentiation of human umbilical cord derived stem cells into endothelial cells. *J Cell Biochem*. 2007;100(3):608–616.
8. Vater C, Kasten P, Stiehler M. Culture media for the differentiation of mesenchymal stromal cells. *Acta Biomater*. 2011;7(2):463–477.
9. Conconi MT, Burra P, Di Liddo R, et al. CD105(+) cells from Wharton's jelly show *in vitro* and *in vivo* myogenic differentiative potential. *Int J Mol Med*. 2006;18(6):1089–1096.
10. Mitchell KE, Weiss ML, Mitchell BM, et al. Matrix cells from Wharton's jelly form neurons and glia. *Stem Cells*. 2003;21(1):50–60.
11. Shetty P, AM Thakur, Viswanathan C. Dopaminergic cells, derived from a high efficiency differentiation protocol from umbilical cord derived mesenchymal stem cells, alleviate symptoms in a Parkinson's disease rodent model. *Cell Biol Int*. 2013;37(2):167–180.
12. Li D, Chai J, Shen C, et al. Human umbilical cord-derived mesenchymal stem cells differentiate into epidermal-like cells using a novel co-culture technique. *Cytotechnology*. 2014;66(4):699–708.
13. Campard D, Lysy PA, Najimi M, et al. Native umbilical cord matrix stem cells express hepatic markers and differentiate into hepatocyte-like cells. *Gastroenterology*. 2008;134(3):833–848.
14. Anzalone R, Lo Iacono M, Corrao S, et al. New emerging potentials for human Wharton's jelly mesenchymal stem cells: immunological features and hepatocyte-like differentiative capacity. *Stem Cells Dev*. 2010;19(4):423–438.
15. Snykers S, De Kock J, Tamara V, et al. Hepatic differentiation of mesenchymal stem cells: *in vitro* strategies. *Methods Mol Biol*. 2011;698:305–314.
16. Nekanti U, Rao VB, Bahirvani AG, et al. Long-term expansion and pluripotent marker array analysis of wharton's jelly-derived mesenchymal stem cells. *Stem Cells Dev*. 2009;19(1):117–130.
17. Nekanti U, Rao VB, Bahirvani AG, et al. Long-term expansion and pluripotent marker array analysis of Wharton's jelly-derived mesenchymal stem cells. *Stem Cells Dev*. 2010;19(1):117–130.
18. Kouroupis D, Churchman SM, English A, et al. Assessment of umbilical cord tissue as a source of mesenchymal stem cell/endothelial cell mixtures for bone regeneration. *Regen Med*. 2013;8(5):569–581.
19. Bongso A, Fong CY. The therapeutic potential, challenges and future clinical directions of stem cells from the Wharton's jelly of the human umbilical cord. *Stem Cell Rev*. 2013;9(2):226–240.
20. Liu S, Yuan M, Hou K, et al. Immune characterization of mesenchymal stem cells in human umbilical cord Wharton's jelly and derived cartilage cells. *Cell Immunol*. 2012;278(1–2):35–44.
21. Weiss ML, Troyer DL. Stem cells in the umbilical cord. *Stem Cell Rev*. 2006;2(2):155–162.
22. Fong CY, Chak LL, Biswas A, et al. Wharton's jelly stem cells have unique transcriptome profiles compared to human embryonic stem cells and other mesenchymal stem cells. *Stem Cell Rev*. 2011;7(1):1–16.
23. Chang YJ, Shih DT, Tseng CP, et al. Disparate mesenchyme-lineage tendencies in mesenchymal stem cells from human bone marrow and umbilical cord blood. *Stem Cells*. 2006;24(3):679–685.
24. Neuss S, Becher E, Wöltje M, et al. Functional expression of HGF and HGF receptor/c-met in adult human mesenchymal stem cells suggests a role in cell mobilization, tissue repair, and wound healing. *Stem Cells*. 2004;22(3):405–414.
25. Neuss S, Apel C, Buttler P, et al. Assessment of stem cell/biomaterial combinations for stem cell-based tissue engineering. *Biomaterials*. 2008;29(3):302–313.
26. Neuss S, Stainforth R, Salber J, et al. Long-term survival and bipotent terminal differentiation of human mesenchymal stem cells (hMSC) in combination with a commercially available three-dimensional collagen scaffold. *Cell Transplantation*. 2008;17(8):977–986.
27. Schneider RK, Neuss S, Stainforth R, et al. Three-dimensional epidermis-like growth of human mesenchymal stem cells on dermal equivalents: contribution to tissue organization by adaptation of myofibroblastic phenotype and function. *Differentiation*. 2008;76(2):156–167.
28. Van de Kamp J, Jahnen Dechent W, Rath B, et al. Hepatocyte growth factor-loaded biomaterials for mesenchymal stem cell recruitment. *Stem Cells Int*. 2013;2013(2013):9.

29. Wang HS, Hung SC, Peng ST, et al. Mesenchymal stem cells in the Wharton's jelly of the human umbilical cord. *Stem Cells*. 2004;22(7):1330–1337.
30. Pittenger MF, Mackay AM, Beck SC, et al. Multilineage potential of adult human mesenchymal stem cells. *Science*. 1999;284(5411):143–147.
31. Can A, Karahuseyinoglu S. Concise review: human umbilical cord stroma with regard to the source of fetus-derived stem cells. *Stem Cells*. 2007;25(11):2886–2895.
32. Dominici M, Le Blanc K, Mueller I, et al. Minimal criteria for defining multipotent mesenchymal stromal cells. The International Society for Cellular Therapy position statement. *Cytotherapy*. 2006;8(4):315–317.
33. Acloque H, Adams MS, Fishwick K, et al. Epithelial–mesenchymal transitions: the importance of changing cell state in development and disease. *J Clin Invest*. 2009;119(6):1438–1449.
34. Yannarelli G, Pacienza N, Cuniberti L, et al. Brief report: The potential role of epigenetics on multipotent cell differentiation capacity of mesenchymal stromal cells. *Stem Cells*. 2013;31(1):215–220.
35. Silva J, Nichols J, Theunissen TW, et al. Nanog is gateway to the pluripotent ground state. *Cell*. 2009;138(4):722–737.
36. Schmitz G, Müller G. Structure and function of lamellar bodies, lipid–protein complexes involved in storage and secretion of cellular lipids. *J Lipid Res*. 1991;32(10):1539–1570.